Evaluating the Thermal Impacts of Different Masonry Wall Tie Designs Using FEM

Yue Shao[1], Maysoun Ismaiel[2], Yuxiang Chen[3]

[1] MSc student, University of Alberta, Department of Civil and Environmental Engineering, Edmonton, Alberta, Canada, yueshao@ualberta.ca

[2] Ph.D. student, University of Alberta, Department of Civil and Environmental Engineering, Edmonton, Alberta, Canada, ismaiel@ualberta.ca

[3]Assistant Professor, University of Alberta, Department of Civil and Environmental Engineering, Edmonton, Canada, yuxiang.chen@ualberta.ca

Abstract

Masonry wall ties is one of the main thermal bridging sources in masonry exterior walls. Traditional steel masonry veneer ties cause a significant reduction in the overall thermal resistance of the masonry walls. Research shows that tie material, shape and spacing have a significant impact on the overall thermal resistance. This study aims to observe the reduction effect of the masonry ties on the thermal resistance of exterior masonry walls and presents viable solutions. Finite Element Models (FEM) are used in this study to compare the effects of different tie spacing, shapes and dimensions on the overall thermal resistance of masonry walls. In addition, this study suggests new insulation schemes by using thermal breakers at the ties' edges to improve the thermal resistance of masonry ties and reduce the thermal bridging effect. Results showed that reducing the length or putting thermal breaker at the interior ends of the ties significantly reduces the thermal bridging impact.

Introduction

Significant amounts of energy are consumed for home heating, cooling, and ventilation purposes. The building energy consumption in Canada accounts for 28% of Canada's secondary energy. Space heating is the major subsector in both residential and commercial buildings, 61% and 55% respectively (NRC, 2014). Therefore, improvements in the energy efficiency of Canadian dwellings have become a focus. Reducing the energy use of space heating in a building is an effective method to decrease the national energy consumption of Canada. Building energy codes require building designers to improve the thermal resistance values of the walls to comply with continuously evolving energy code requirements.

Masonry walls can provide excellent thermal resistance and also have good durability and architectural appearance. The superior physical properties of masonry can improve the thermal performance of exterior walls and reduce energy consumption to keep a comfortable living environment. However, thermal bridging is one of the main challenges facing the thermal performance of masonry walls. Thermal bridges in building envelopes occur mostly in places where structural components with high conductivity penetrate the thermal insulation layers. In the case of masonry walls, this phenomenon occurs through the ties, hangers, shelf angles, and insulation fasteners. The masonry ties' function in masonry cavity walls is to connect multiple wythes of masonry and provide horizontal structural supports. The tie material and tie design can have a significant impact on the effective thermal resistance (R-value) of masonry walls; the effective reduction can range from 3% to 25%, depending on the thickness of the insulation and the materials thermal properties (Wilson and Higgins, 2014). Suggestions of the tie improvement can guide the manufacturing companies to optimize and develop their products. Therefore, research on the impact of masonry ties on the thermal performance of masonry exterior walls is necessary and will improve the efficiency of energy use in buildings and promote sustainable developments.

There has been an evolution in the shapes, sizes, materials, and configuration of the ties to improve thermal performance. Several tie types with different materials were introduced to the market to lower the thermal bridging reduction effect on the overall thermal resistance. These include unit ties, adjustable ties, and re-anchoring systems (The Brick Industry Association, 2003). The adjustable ties are more convenient for construction than the unit ties. One of the most common adjustable tie types is the slotted ties; the presence of holes through the body of the tie reduces the cross-sectional area, thus decreasing thermal conductance through the tie system. Literature showed that the slotted ties have the highest thermal efficiency compared to the other tie types (Fero, 2015). Therefore, the slotted ties are the focus of this study.

Although several previous studies have discussed the effect of using different ties' materials, little analytic attention has been paid to the impact of varying tie design configurations. This study focuses on the slotted tie type and uses FEM to investigate the impact of some variables such as the ties' spacing, shape and dimensions on the overall thermal resistance of the masonry walls. Furthermore, two insulation schemes are introduced by using thermal breakers at the ties' edges to improve the thermal performance of masonry ties and reduce the thermal bridging effect. With a clear understanding of the impact of masonry ties, better masonry wall designs can be achieved.

This study has been developed through the following steps. First, an introduction provides a brief background of the masonry walls and ties. Also, the introduction presents the objectives and motivations of this study. Then, the methodology of modelling is presented in the numerical simulation section. Followed by the results and discussion. Finally, the conclusion section summarizes the key findings derived from this study and recommendations for future research are presented.

Numerical simulation

Different heat transfer mechanisms are initiated through the wall assembly due to the presence of airflow within; (1) the cavity wall between the brick veneer and insulation boards, (2) airflow within a concrete unit's cores, and (3) the temperature gradient across the depth of concrete masonry units (CMU) cavity walls. Thermo-fluid dynamic behaviour should be considered in the thermal analysis of the concrete masonry cavity walls to assure accurate results (Sun and Fang, 2009; Henrique Dos Santos, Fogiatto and Mendes, 2017; Laaroussi *et al.*, 2017).

The governing equations of fluid dynamics and thermal analysis are: the continuity equations, representing the conservation of mass; the Navier-Stokes equations represent the conservation of momentum; and the first law of thermodynamics equations describes the conservation of energy (Arendt, Krzaczek and Florczuk, 2011). These governing equations are nonlinear partial differential equations that can be solved using a finite element simulation program ANSYS Workbench 2019-R3 (ANSYS Inc, 2019).

ANSYS Workbench was used to perform Finite Element Analysis (FEA) of a typical residential brick veneer cavity wall system that has an air cavity behind the brick veneer layer. The wall assembly investigated in this study is a fully grouted masonry wall. The air movement in the cavities between the brick veneer and the insulation panel is assumed to be only driven by natural convection. Figure 1 shows the wall assembly investigated in this study.

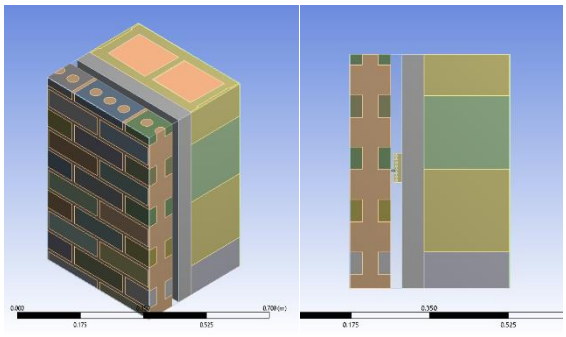

Figure 1: FEM representing the studied wall assembly using ANSYS workbench.

Model description

Several previous studies on the thermal performance of masonry walls used two-dimensional numerical models. There are many investigations considering the thermal bridges and developing statistical models representing the thermal transmittance of 2-D thermal bridges (Salgon and Neveu, 1987; Déqué, Ollivier and Roux, 2001; Larbi, 2005; Gao *et al.*, 2008). The two-dimensional modelling approach provides some preliminary information on the effect of the thermal bridge on the energy performance of buildings. However, to assess the thermal performance of CMUs cavity walls with high accuracy, three-dimensional models with accurate thermal boundary conditions should be considered (Hassid, 1990; Can et al, 2003). Accordingly, this study developed three-dimensional numerical models to evaluate the R-values of the cavity walls. A total of nine FEMs were constructed. One model is considered the base model without any ties added (reference model). This model is used for comparison purposes only. Three groups were addressed to discuss different variables: group (1) presents different tie configuration and shape (four models), group (2) presents different tie spacing defined by centreline between ties (two models), and finally, group (3) presents assemblies with thermal breakers at the edges of the tie (two models).

All tie types used in this study are presented in Table 1, as well as the different variables considered in each group. The type of ties used in the models discussing the tie spacing (group 2) and the thermal breaks (group 3) are tie #1 with dimensions (184× (50+25)) mm as shown in Figure 2. For illustration, Figure 2 shows the tie types used in this investigation with dimensions. The four ties, #1 to #4 considered in this study, have the same surface area. Tie #1 is one of the most common shapes of ties used in Alberta. The different tie spacing usually used in the assemblies in construction (centreline dimensions) are shown in Figure 3. The configurations of the thermal breakers are shown in Figure 4.

The models were analyzed in steady-state conditions. Conductive, convective, and radiation heat transfer are considered within each wall system. The numerical models were developed using mixed convective and radiation boundary conditions to simulate the external environment and the air cavity boundary conditions. Three boundary conditions were employed: (1) temperatures for the indoor and outdoor conditions, (2) emissivity, and (3) heat transfer coefficients.

Table 1: Variable schemes

	Variables discussed	**Descriptions**
Group (1)	Ties	Tie#1:(184×(50+25)) mm
		Tie#2:(184×75) mm
		Tie#3: (171×75) mm
		Tie#4: (120×110) mm
Group (2)	Total specimen dimensions (Using Tie#1)	400×400×355 mm
		400×600×355 mm
Group (3)	Thermal breaking configurations (Using Tie #1)	Tie whole insulation
		Tie ¼ insulation

Considering the literature survey (ASTM C1058, 2015), the temperatures applied in this model are $T_{outdoor}$ = -20°C and T_{indoor} = 24°C, were the temperatures of the outdoor and indoor environment in contact with the face surface

of the brick veneer and CMU backup wall, as shown in Figure 5.

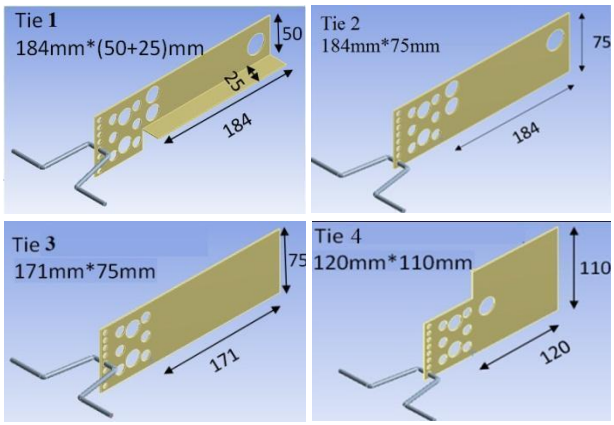

Figure 2: Different ties configurations-shapes of ties (group 1)

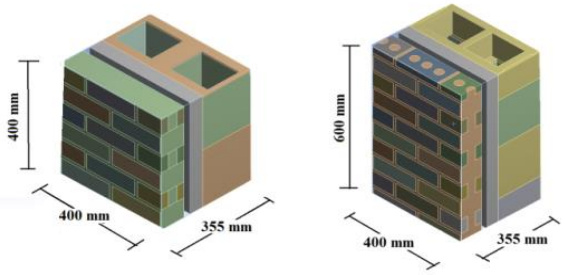

Figure 3: The different tie spacing (group 2).

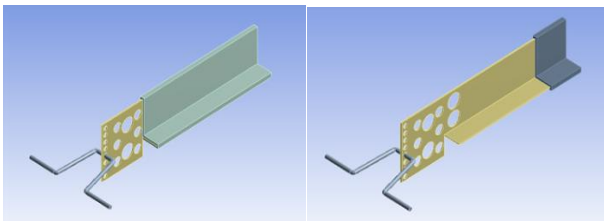

Figure 4: The different thermal breaking configurations. Whole tie insulation and ¼ tie insulation respectively (group 3).

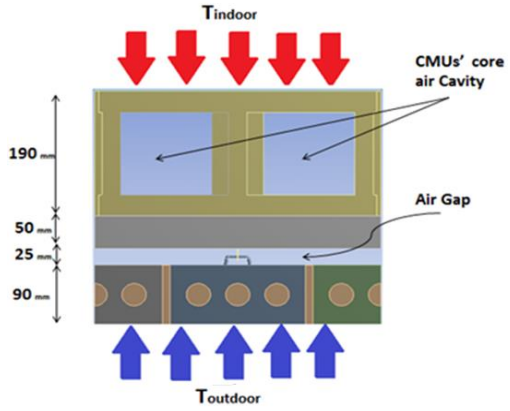

Figure 5: The temperatures of the indoor and outdoor in contact with the face surface of the CMU.

The thermal transmittance evaluation of hollow blocks is required to simulate accurate modelling. Previous studies showed the importance of including the three heat transfer mechanisms and considering the influence of airflow within the cells of the masonry units to simulate an effective numerical model (Mooneghi, Kargarmoakhar and Chowdhury, 2015; Martínez *et al.*, 2018).

There are many empirical correlations for convective heat transfer across a rectangular cavity. ElSherbiny, Raithby and Hollands (1980) discussed the heat transfer by natural convection across vertical and inclined air layers. Based on the following equations, the convective heat transfer coefficient of the 25 mm air gap between the brick veneer and the insulation layer is chosen to be h_c= 1.41 W/m^{2}K The convective heat transfer is coupled with surface temperatures and other parameters. The actual values of "h" varies slightly for different configurations. For this study, they are chosen to be constant.

$$T_m = \frac{T_{indoor} + T_{outdoor}}{2} \quad (1)$$

$$a = \frac{100}{T_m} \quad (2)$$

$$k_{air} = \frac{0.002528 \times {T_m}^{1.5}}{T_m + 200} \quad (3)$$

$$R_a = 2.737 \times (1 + 2a)^2 \, a^4 \, (T_{indoor} - T_{outdoor}) \left(\frac{L_{cavity}}{mm}\right)^3 P^2 \quad (4)$$

$$N_{ul1} = 0.0605 \times (R_a)^{\frac{1}{3}} \quad (5)$$

$$N_{ul2} = \left[1 + \frac{0.104 \times (R_a)^{0.293}}{\left(1 + \left(\frac{6310}{R_a}\right)^{1.36}\right)^3}\right]^{\frac{1}{3}} \quad (6)$$

As $N_{ul1} > N_{ul2}$ then the convective heat transfer is considered as follow;

$$h_c = \frac{k_{air}}{L_{cavity}} \quad (7)$$

Where: T_m is the temperature measured in (K), T_{indoor} is the temperature for the indoor environment (K), $T_{outdoor}$ is the temperature for the outdoor environment (K), k_{air}: thermal conductivity of air (W/m·K), R_a: Rayleigh number, N_{ul}: Nusselt number, h_c: the convective heat transfer coefficient of the air gap (W/m^{2}K) and L_{cavity} is the air cavity thickness (m). Finally, adiabatic boundaries were applied to the side, top and bottom surfaces of the assemblies to avoid any heat flow losses at the edges.

Meshing was done by using ANSYS's advanced sizing feature. The software can generate a relatively fine mesh for each part in the model without setting a global size criterion. This is a significant feature as some wall components as the ties are relatively thin and need more elements and refined mesh, while the blocks, the brick veneer and the insulation boards used do not need the same size elements to resolve heat flow through them accurately. The mesh of the cavity wall assembly is shown in Figure 6.

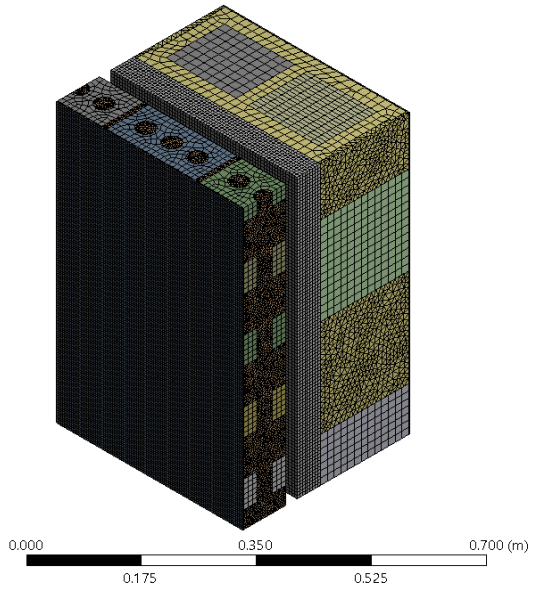

Figure 6: Cavity wall assembly mesh

Material properties

There are some modelling assumptions considered in this study; the exterior surface-air-film is not considered in the modelling. The air density within the cavities was assumed to be constant. Heat flow and surface temperatures reached constant values (i.e., steady-state conditions). The thermal properties for each component were determined based on the common material properties in Canada and the literature survey.

According to the existing literature, the typical values for the external emissivity of masonry surfaces range between 0.85 and 0.95 (ASHRAE, 2017; Li *et al.*, 2008; Henrique Dos Santos, Fogiatto and Mendes, 2017). The emissivity values used in this modelling and the material properties used in this study are listed in Table 2.

Table 2: Thermal Properties of Wall Components.

Material	Density (kg/m^3)	Thermal Conductivity (W/(m·K))	Specific Heat (J/(kg·K)	Emissivity
Air	1.225	0.0242	1006.4	-
Brick	1900	0.72	835	0.93
Concrete	2300	0.72	780	0.85
Mortar	1860	0.72	780	0.87
Polyurethane foam, rigid	192	0.0444	1550	0.855
Stainless steel, forties	7750	24.9	474	0.6

Conductive, convective and radiation heat transfer were simulated simultaneously by using ANSYS. All assemblies have the same total thickness of 355 mm. The size of the brick unit is 190mm×90mm×57mm while CMU is standard CMU, 390mm×190mm×190mm. The thicknesses of each wall component considered in the simulation are shown in Figure 5. Additionally, the material of the tie thermal breaker is the same as the insulation board, and the thickness of the thermal breaks around the main surfaces of the tie is 2.25mm while the thickness is 6mm at the end of the tie.

The simulated overall R-values, or called effective R-values (R_{eff}), were calculated for all assemblies using equation (8):

$$R_{eff} = \frac{\Delta T}{q} \quad (8)$$

Where R_{eff} is the effective thermal resistance (m^{2}K/W), ΔT is the difference in surface temperature across the studied specimen (K), and q is the average heat flux (W/m^2) measured from the finite element simulation results.

Results and Discussion

To compare the impact of using different ties on the overall thermal performance of cavity walls, a base assembly was simulated with no ties to represent the reference assembly. The results will be discussed and presented for the three main groups: group (1) presents the comparison results between different ties (Ties 1, 2, 3, and 4) as described previously in Table 1; group (2) presents the effect of different dimensions and ties distribution on the overall thermal performance; and group (3) presents the effect of using two configurations of tie's thermal breaks. All cases studied and mentioned above are fully grouted.

Group (1): Effect of ties' shape and dimension

The results show that assembly with tie #4 has the best thermal resistance, where the thermal resistance is lower than the reference case (no tie) by 4.4%. Figure 7 shows the temperature distribution for each tie type and the side view of the temperature distribution of the tie penetrating the insulation panel.

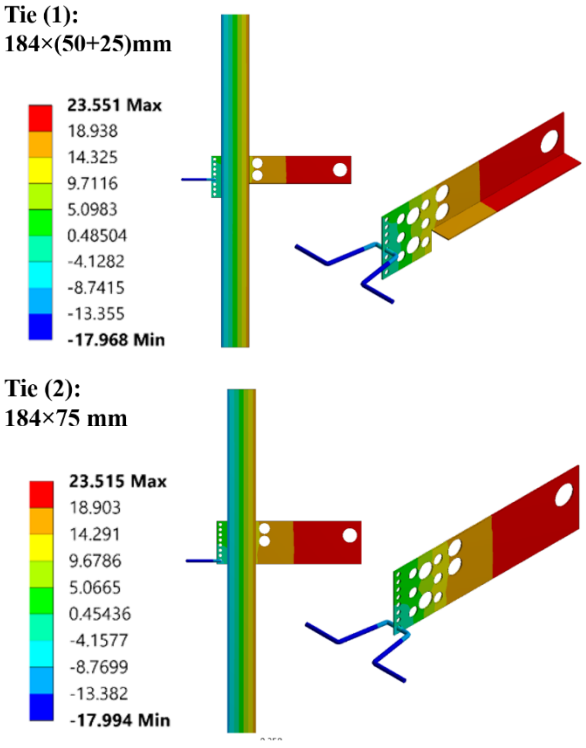

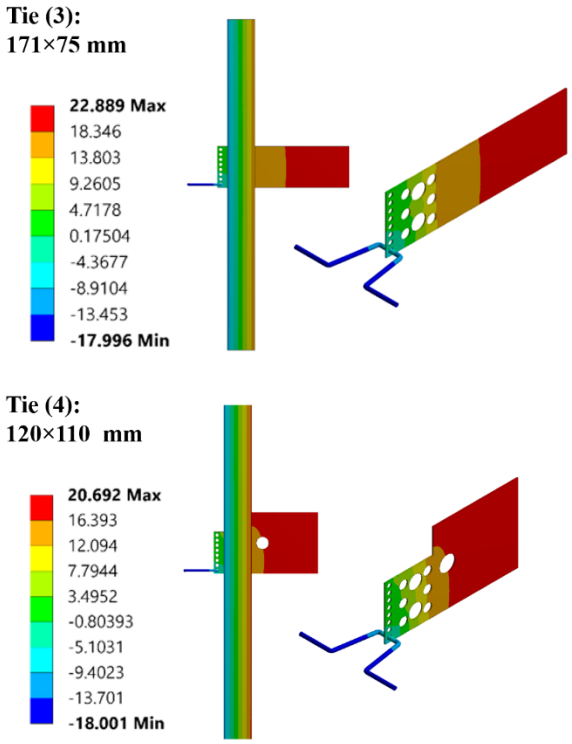

Figure 7: Temperature distribution- Side view with the insulation panel and the tie isometric view (℃).

Figure 8 shows the thermal resistance of the overall four tie type assemblies. Table 3 shows the differences between the total heat flux value of each case and the reference case (no-tie), as well as the overall resistance values of each case and no-tie case.

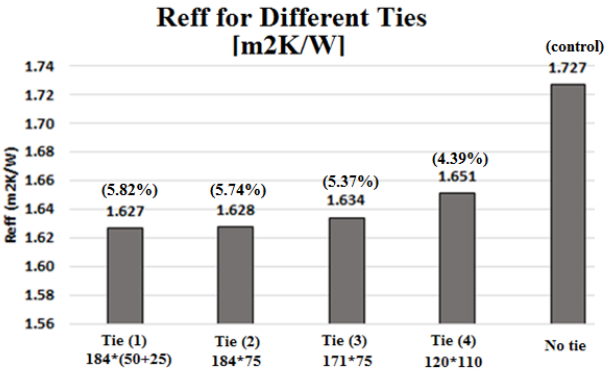

Figure 8: R_{eff} values of the four assemblies and the no ties case as well as the reduction % in the R_{eff} value for each case.

The heat flux was investigated on both sides, the inner CMU and the outer brick veneer. Figure 9 shows the heat flux distribution on both sides in each case.

The shape of the tie does not affect the R_{eff} value of the wall if they have the same depth and same surface area (different shapes of cross-section). Figure 9 shows that tie #1 has the highest heat flux value. The angle part (25mm) presented in tie #1 has no significant effect. Table 3 shows simulation results for all studied ties.

In addition, results show that the penetration depth of the tie into the interior CMU backup wall affects the R_{eff} value of the wall significantly. All the ties have the same surface area; however, a significant change in the total heat flux values was observed through the specimens and the R_{eff} value of the wall, as shown in Table 3. The reduction of R_{eff} in case of using tie#4 is 1.35% less than tie#1. Also, Figure 9 shows that the maximum heat flux value occurs when the end of the tie is closer to the inner CMU backup wall surface.

Table 3: The differences between the overall resistance values of each case and the no-tie case (reference model).

Assembly description	Average total heat flux value of CMU surface (W/m2)	R_{eff} (m^2K/W)	Reduction (%)
Tie #1 (184×(50+25))	27.049	1.627	5.82
Tie #2 184×75	27.028	1.628	5.74
Tie #3 171×75	26.922	1.634	5.37
Tie #4 120×110	26.647	1.651	4.39
No tie	25.476	1.727	Reference

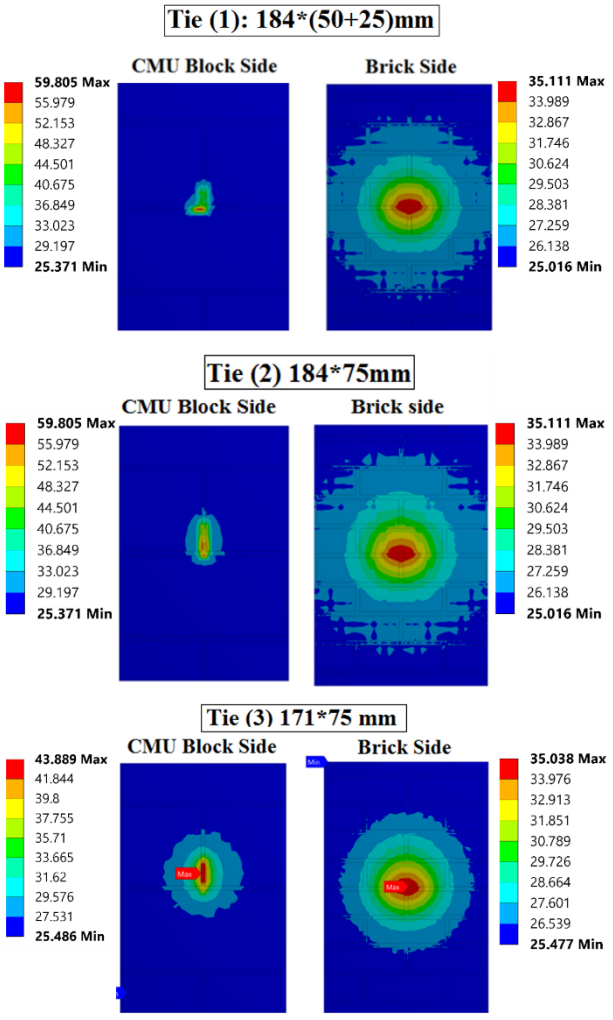

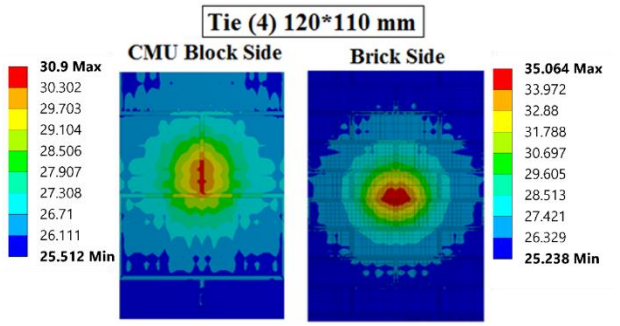

Figure 9: Heat flux distribution on both walls surfaces (Outer and inner) (W/m^2).

Group (2): Effect of ties' spacing

Results showed that the ties' spacing change caused a reduction in the overall resistance value by about 1.8%~2.2%. Figure 10 shows the difference between the 400×400 mm, 400×600 mm and the reference case (no-tie).

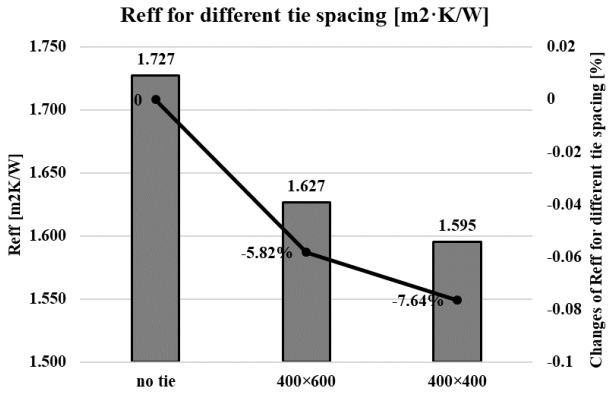

Figure 10: Effect of ties spacing

Group (3): Effect of using thermal breaks

Figure 11 shows the variations of the overall resistance values in case of using thermal breaks and the percentage change in the R_{eff} value for each case. Table 4 shows the R-effective values for each case as well as the heat flux on the inner surface of the wall. While Figure 12 shows the heat flux distribution on both wall surfaces in the two insulation cases.

Based on the results of the heat flux distribution shown in Figure 12, as well as the total heat flux values and R_{eff} values presented in Table 4, it was concluded that the lowest resistance is for the uninsulated ties, which have an overall resistance reduction value of 5.8% with respect to the no tie case. While the ¼ insulation ties had almost similar total thermal resistance to the full insulation case. The reduction value of the overall thermal resistance of the ¼ insulated ties assembly was found 2.3% with respect to the no tie case, while the assembly with fully insulated ties is 2.5%. However, some construction aspects that should be considered in case of using ties thermal breaks, for ¼ insulation ties, the risk of tie slipping out of the insulation enclosure is greatly reduced compared to the fully insulated tie scenario because the contact area of the ties with mortar increases significantly.

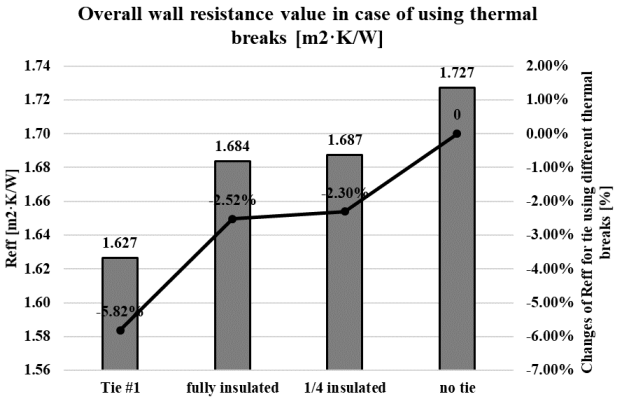

Figure 11: The variations of the overall resistance values in case of using thermal breaks as well as the changes % in the Reff value for each case.

Table 4: The heat flux for surface inner Concrete masonry blocks in case of using thermal break.

Assembly description	Heat flux value (CMU surface) (W/m^2)	R_{eff} (m^2·K/W)	R-value Reduction (%)
No tie	25.476	1.73	Reference
Tie #1	27.049	1.63	5.8
Fully insulated	26.134	1.68	2.5
1/4 insulated	26.077	1.68	2.3

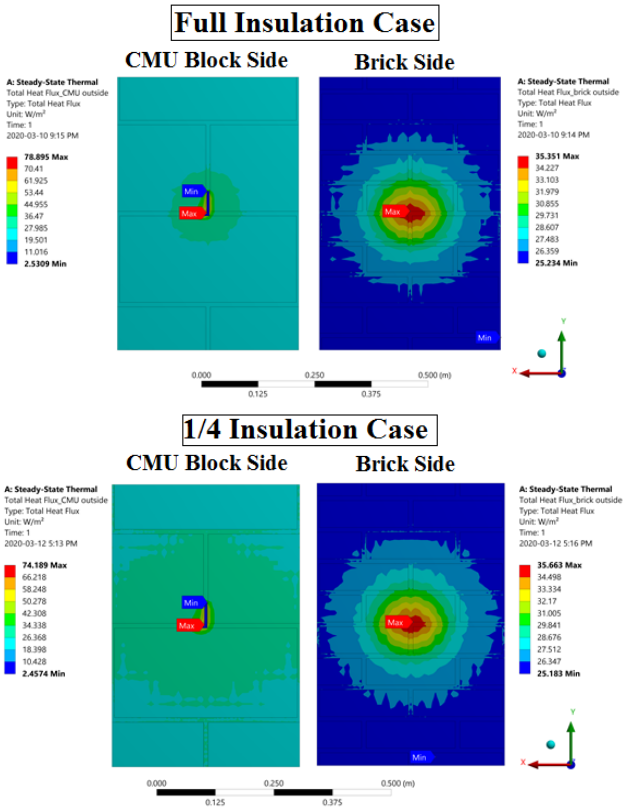

Figure 12: Heat flux distribution on both walls' surfaces (Outer and inner) in case of using thermal breaks around the ties.

Conclusion

The conclusion of this study is summarized as follows; the four studied cases of ties showed a reduction in the overall resistance values of the assemblies that could reach 6%. One of the main reasons for R_{eff} reduction is the depth of the tie in the backup wall. When ties have the same surface area and material, the thermal resistance reduction from full length (Tie #1) to 2/3 backup wall depths (Tie #4) decreases by 1.4% of no-tie case.

The comparison between different tie spacing showed an impact on the overall resistance value. It reduced the R-effective by 1.8% when vertical spacing changes from 600mm (3 blocks height) to 400mm (2 blocks height). For improving the thermal resistance of masonry walls, it is recommended to use large tie spacing in construction.

Using thermal breaks around the ties proved that it had a positive impact on the overall thermal resistance. And using ¼ insulation is more cost-performance than using fully wrapped insulation. Using thermal breaks can increase the thermal resistance of the wall by more than 3% compared to commonly used ties (tie #1). In other words, the effective thermal resistance of the insulated tie scenario only decreases the R_{eff} value by 2.5% compared to the no tie case (reference assembly). Finally, it was concluded that adding an insulated panel around the end of the tie reduces the thermal bridging impact of the ties on the masonry wall assembly.

Future recommendations

This study is limited to the thermal properties of fully grouted unvented masonry cavity walls, in other words, all convective heat transfer in the air cavities in the modelling is natural convection. Further investigations will be required to focus on the vented masonry cavity wall and hollowed masonry wall blocks. In addition, estimation of the thermal impact of the air velocity inside the air gap on the masonry cavity wall assemblies is required to be addressed further. Also, experimental investigations are significant and required for verification purposes and improvements of the finite element simulations.

References

Arendt, K., Krzaczek, M., & Florczuk, J. (2011). Numerical analysis by FEM and analytical study of the dynamic thermal behavior of hollow bricks with different cavity concentration. *International Journal of Thermal Sciences*, *50*. 1543-1553.

ANSYS Inc (2019). https://www.ansys.com/about-ansys.

ASHRAE (2017) 'Heat, air, and moisture control in building assemblies - Material properties', *ASHRAE handbook - Fundamentals*, p. 22.

ASTM International. (2015). *ASTM C1058: Standard Practice for Selecting Temperatures for Evaluating and Reporting Thermal Properties of Thermal Insulation*. *ASTM International*, (*10*, *1–4*).

Can A., Buyruk E., Can Y. (2003). Heat Bridges Effects on Heat Loss and Heat Gain at Buildings. *13th International Conference on Thermal Engineering and Thermogrammetry (THERMO)*, Budapest (Hungary) 2003, 81-86.

Déqué, F., Ollivier, F., & Roux, J. J. (2001). Effect of 2D modelling of thermal bridges on the energy performance of buildings - Numerical application on the Matisse apartment. *Energy and Buildings*, *33*, 583–587.

ElSherbiny, S. M., Raithby, G. D., & Hollands, K. G. T. (1980). Heat Transfer By Natural Convection Across Vertical and Inclined Air Layers. *American Society of Mechanical Engineers (Paper)*, *104*(80-HT-67).

Fero Corporation (2015). *Block shear connector*.

Gao, Y., Roux, J. J., Zhao, L. H., & Jiang, Y. (2008). Dynamical building simulation: A low order model for thermal bridges losses. *Energy and Buildings*, *40*, 2236–2243.

Hassid, S. (1990). Thermal bridges across multilayer walls: An integral approach. *Building and Environment*, *25*(2), 143–150.

Henrique Dos Santos, G., Fogiatto, M. A., & Mendes, N. (2017). Numerical analysis of thermal transmittance of hollow concrete blocks. *Journal of Building Physics*, *41*(1), 7–24.

Laaroussi, N., Lauriat, G., Raefat, S., Garoum, M., & Ahachad, M. (2017). An example of comparison between ISO Norm calculations and full CFD simulations of thermal performances of hollow bricks. In *Journal of Building Engineering*, *11*, 69-81.

Larbi, A. Ben. (2005). Statistical modelling of heat transfer for thermal bridges of buildings. *Energy and Buildings*, *37*, 945–951.

Li, L. P., Wu, Z. G., Li, Z. Y., He, Y. L., & Tao, W. Q. (2008). Numerical thermal optimization of the configuration of multi-holed clay bricks used for constructing building walls by the finite volume method. *International Journal of Heat and Mass Transfer*, *51*, 3669–3682.

Martínez, M., Huygen, N., Sanders, J., & Atamturktur, S. (2018). Thermo-fluid dynamic analysis of concrete masonry units via experimental testing and numerical modeling. *Journal of Building Engineering*, *19*, 80–90.

Mooneghi, M. A., Kargarmoakhar, R., & Chowdhury, A. . (2015). Improving the Thermal Performance of Concrete Masonry Blocks. *ASCE Florida Section 2015 Annual Conference Proceedings*.

Natural Resources Canada (2014). *Canada's Secondary Energy Use by Sector, End-Use and Subsector, Energy Use Data Handbook Tables*.

Salgon, J. J., & Neveu, A. (1987). Application of modal analysis to modelling of thermal bridges in buildings. *Energy and Buildings*, *10*(2), 109–120.

Sun, J., & Fang, L. (2009). Numerical simulation of concrete hollow bricks by the finite volume method. *International Journal of Heat and Mass Transfer*, *52*(23–24), 5598–5607.

The Brick Industry Association (2003). *Technical Notes 44B - Wall Ties for Brick Masonry*.

Wilson, M., & Higgins, J. (2014). Fero rap tie and fast system thermal analysis. *RDH Building Engineering Ltd. Vancouver (Canada).*